Journal Name

Dynamic Article Links ►

Cite this: DOI: 10.1039/c0xx00000x

www.rsc.org/xxxxxx

ARTICLE TYPE

Functionalized Large Pore Mesoporous Silica Nanoparticles for Gene Delivery Featuring Controlled Release and Co-delivery †

Sandy Budi Hartono,[a] Nghia Truong Phuoc,[a] Meihua Yu,[a] Zhongfan Jia,[a] Michael Monteiro,*[a] Shizhang Qiao ,*[b] Chengzhong Yu*[a]

Received (in XXX, XXX) Xth XXXXXXXXX 200X, Accepted Xth XXXXXXXXX 200X

DOI: 10.1039/b000000x

Novel mesoporous silica nanoparticles (LPMSN) functionalied with degradable poly(2-dimethylaminoethyl acrylate) (PDMAEA) have been developed (PDMAEA-LPMSN) as nano-carriers for gene delivery. The unique design of PDMAEA-LPMSN has endowed this system with multifunctions derived from both the organic and inorganic moieties. The cationic polymer unit binds to genetic molecules and undergoes a self-catalyzed hydrolysis in water to form a non-toxic anionic polymer poly(acrylic acid), allowing controlled release of siRNA in the cells. The nanopores of LPMSN provide a reservoir for storage and release of chloroquine to facilitate endosome escape. The PDMAEA-LPMSN composites were characterized by elemental analysis (EA), X-ray photoelectron spectroscopy (XPS), solid-state 13C magic-angle spinning nuclear magnetic resonance (MAS-NMR), thermogravimetric analysis (TGA), and nitrogen sorption techniques. Their siRNA delivery performance was tested in a KHOS cell line, showing promising potential for the co-delivery of genes and drugs.

Introduction

Small interfering RNA (siRNA) based therapeutics has received increasing attention for cancer treatment applications.[1] The siRNA therapy features highly specific siRNA to silence oncogenes. However, the vulnerability of siRNA against nuclease and the poor cellular delivery hampers its *in vivo* application.[2] Nanocarriers that can package, protect and deliver siRNA to the targeted site hold promise to solve these problems for the practical applications of siRNA therapy.[3]

Various nanocarriers have been developed to deliver siRNA, such as lipid and polymer based carriers.[4] Inorganic materials (*e.g*. gold, iron oxide and silica materials) have also been studied as carriers for genetic molecules.[5-8] Recently, mesoporous silica nanoparticles (MSN) based materials showed promising performance as gene carriers. [9-11] Various surface modified MSN have been systematically studied to deliver siRNA. Short amine silane moieties have been extensively used to increase silica affinity towards the nucleic acid agents (DNA, siRNA).[9-11] Meng *et al* used polyethyleneimine (PEI) modified MSN with different molecular weights to enhance the efficacy of siRNA.[12] In addition, polyamine dendrimer-MSN have also been used for delivering siRNA.[13] Composite materials consisting of both polymer and mesoporous silica combine the benefits from each component to create a more advanced carrier system.[8, 13, 14] Polycation or polyamine complex with MSN are more versatile compared to the short chain amine-MSN. The presence of multi amine moieties significantly enhances particle affinity towards siRNA and cell membrane. [15]

The main issue related to the polycation complex with siRNA (polyplex) is the strong binding between the abundant positive charge on the polymer and the negatively charged phosphonic acid of the nucleic acid, which hinders the release of siRNA within cytoplasma thus lowering the efficacy of siRNA.[16, 17] This factor is also known as vector unpacking. To exert siRNA function, it needs to be transferred into cytoplasm and released from the carrier as free molecules to induce gene silencing.[18, 19] The second issue is cytotoxicity of polycation.[17] This condition raises a concern about accumulated toxicity of the nanoparticles, especially after multi-administration. Previously, we have reported the use of poly-l-lysine (PLL) functionalised large pore mesoporous silica nanoparticles (LPMSN-P) as gene carriers.[15] PLL-functionalized nanoparticles had a strong binding towards nucleic acid molecules and delivered oligo DNA-Cy3 (a model for siRNA) efficiently to HeLa cells. However, the low release of siRNA from the complex limited the effectiveness of this system.

Degradable polycationic polymers that can be degraded into non-toxic compounds and enhance gene release are preferable as carriers in gene therapy.[16] Several methods have been used to establish degradable structures by introducing cleavable bonds into the polymer structures. The cleavable bonds include esters, amides, carbonates and disulfides. Most of these structures depend on various external triggers (pH, redox potential and enzymes) to start the degradation.[17, 20-22] Yet, the high fluctuation of these triggers within the human body might cause

inconsistency in the cleavage reactions, resulting in variable and unpredictable rates of degradation.[23, 24] It is desirable to use a cleavable polymer that degrades only after being internalized by target cells in a simple and controlled manner.[23, 24]

Recently, a self-catalyzed degradable cationic polymer (poly(2-dimethylaminoethyl acrylate), PDMAEA), which degrades independently of an external degradation trigger, has been developed. [23, 24,25] The degradation product is the non-toxic poly(acrylic acid), PAA. The most prominent features of this polymer are the ability to bind and protect oligo-DNA for sufficient times and the capacity to release the DNA inside the cells after 10 hours.[23, 24,25] In this work, we used PDMAEA covalently attached to the surface of large pore mesoporous silica nanoparticles (PDMAEA-LPMSN) to act as a dual delivery system. The surface bound PDMAEA can bind and release siRNA 'on-demand'. Chloroquine was loaded in the nanopores of LPMSN as a model drug which helps endosome escape. It was shown that PDMAEA-LPMSN released oligo-DNA (mimicking siRNA) within 2 days of incubation, while little release was observed in polyethyleneimine (PEI) functionalized LPMSN. In the delivery of a functional siRNA (PLK1), chloroquine loaded PDMAEA-LPMSN inhibited the viability of KHOS cancer cells significantly compared to PDMAEA-LPMSN, showing the advantage of a carefully designed composite co-delivery system.

Experimental section

Chemicals

Triblock poly(ethylene oxide)-b-poly(propylene oxide)-b-poly (ethylene oxide) copolymer $EO_{106}PO_{70}EO_{106}$ (Pluronic F127, MW=13400), fluorocarbon surfactants (FC-4), tetraethoxysilane (TEOS, 99%), 1,3,5-trimethylbenzene (TMB), Copper(I) bromide ,3-glycidoxypropyl trimethoxysilane (3-GPS), 3-aminopropyltriethoxysilane (APTES, 99%), sodium azide, ethyl 2-chloropropionate (97%), copper powder (size <425 µm, 99.5% trace metals basis), tris[2-(dimethylamino)ethyl]amine were used as received from Sigma Aldrich. 2-(dimethylamino) ethyl acrylate (98%), N,N-Dimethylacrylamide (99%) were passed through a column of basic alumina to remove inhibitor before use. N-hexane (>98%), dichloromethane (99.8%), and methanol (99.8%) were used as received from Merck. Polyethyleneimine (PEI) (MW: 10 kDa) were purchased from Alfa Aesar (Ward Hill, MA). All chemicals were used as received without purification. Cell lines used: osteosarcoma cell line KHOS/NP (CRL-1544™) were purchased from ATCC (American Type Culture Collection). Twenty-one-nucleotide (oligo) DNA conjugated with cyanine dye (Cy-3), fetal calf serum, paraformaldehyde and anti-fade fluorescent mounting medium with 4'-6-Diamidino-2-phenylindole (DAPI) were purchased from Sigma Aldrich. Dulbecco's Modified Eagle's Medium (DMEM) and Penicillin G, streptomycin sulphate and L-Glutamine mixture were from Gibco-Invitrogen. CellTiter-Glo® cell viability assay kit was from Promega. Synthetic human PLK1 were purchased from Ambion at Applied Biosystems (Foster City, CA). The siRNA sequences are: PLK-S: 5'-CCAUUAACGAGCUGCUUAATT-3'; PLK-AS: 5'-UUAAGCAGCUCGUUAAUGGTT-3'. S10-siRNA was synthesized by Proligo (Lismore, Australia) and the sequence: S10-S: 5'-GCAACAGUUACUGCGACGUUU-3'; S10-AS: 5'-ACGUCGCAGUAACUGUUGCUU- 3'.

Synthesis of LPMSN

LPMSN were synthesised following a previous method by Ying *et al*.[26] First, 0.5 g F127 and 1.4 g of FC-4 were dissolved in 60 ml of 0.02 M HCl and stirred for 24 hours at 60 ºC. 0.4 g of TMB was added into the mixture and stirred at a temperature of 30 ºC for 6 hours. Then, 3 g of TEOS was added to the solution, and the stirring process at 30 ºC was continued for another 24 hours. The solution was then transferred into autoclaves for the hydrothermal treatment. The hydrothermal temperature was at 100 °C for 24 hours. The sample was denoted as as-synthesized LPMSN (AS-LPMSN). The surfactant (F-127) was still remained within the pores of AS-LPMSN.

Synthesis of 2-bromo-N-(3-(triethoxysilyl)propyl)propan-amide

BPB in 50 mL DCM was added dropwise to a cold solution of APTS and TEA in 200 mL dry DCM. The solution was stirred for 30 min at room temperature and the precipitate was filtered off. The solution was washed with acidic water and dried with magnesium sulphate. After filtration the solvent was removed in rotovapor. The product was dried under vacuum for 24 hours.

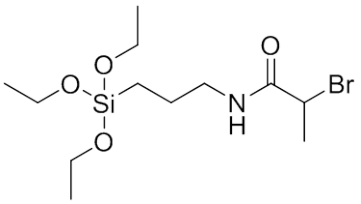

Synthesis of Azidation of 2-bromo-N-(3-(triethoxysilyl)-propyl)propanamide or Azide silane

BPTS was dissolved in dry DMF and NaN_3 was added. The mixture was stirred for 48 hours at room temperature. The solution was then diluted with 200 mL of DCM, washed by water and concentrated by evaporator. The product was dried under vacuum for 24 hours.

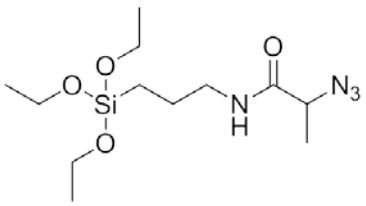

Synthesis of Poly(2-Dimethylaminoethyl Acrylate) (PDMAEA) by SET-LRP [27]

$CuCl_2$/Me_6TREN (32 mg, 8.8 x 10^{-5} mol), Me_6TREN (61 mg, 2.6 x 10^{-4}), ethyl 2-chloropropanoate (120 mg, 8.8 x 10^{-4} mol) and 2-dimethylaminoethyl acrylate (DMAEA, 18.9g, 0.132 mol) were dissolved in isopropanol (10 mL) and the solution was purged argon for 30 minutes at room temperature. Cu powder (size < 425 µm) was added under argon flow. After 7 hours of polymerisation at room temperature, the solution was diluted by acetone (100

mL) and passed through Al_2O_3 to remove copper. Acetone was removed by the rotavap, and the product was obtained by precipitating in a large excess of cold n-hexane (500 mL) and then isolated by centrifugation. This procedure was repeated three times. The polymer was dried under high vacuum for 48 hours at room temperature to give a yellow oily product (yield 70%). The conversion of polymerization was 40 % as determined by ^1H NMR spectroscopy. M_n = 4200, PDI = 1.29 (SEC-RI calibrated using PSTY standards and used DMAc + 0.03 wt% LiCl as eluent).

Synthesis of Azide-MSN (A-MSN), PDMAEA-LPMSN

To establish azide groups on the surface of LPMSN, 5.3 mg 2-azido-N-(3-(triethoxy silyl)propyl)propanamide or azide silane was grafted onto 100 mg AS-LPMSN in 25 ml Toluene. The reaction was maintained at 70 ºC for 24 hours. The product was washed with toluene and methanol and followed by surfactant removal. The surfactant removal was conducted by using an extraction process in acidic-methanol for 24 hours and the process was repeated three times. The product is named A-MSN. A-MSN has an opened pores structure.

Finally, a click reaction between alkynes- poly(2-dimethylaminoethyl acrylate) (PDMAEA) and A-MSN also known as the Huisgen 1,3-dipolar cyclo-addition can be conducted. 100 mg A-MSN and 578 mg PDMAEA was mixed in 2 ml of toluene at a room temperature under argon, followed by addition of 9 µl of PMDETA. Then, 6 mg of copper bromide (CuBr), as a catalyst, was added to the mixture. The reaction was maintained for 24 hours. The product PDMAEA-LPMSN was washed and dried in vacuum.

Synthesis of PEI-LPMSN

At first the epoxysilane was attached on the silica surface: 100 mg of LPMSN was mixed in 30 ml of toluene and stirred for 15 minutes at 70 ºC. 1.5 ml of 3-GPS was added into the solution and further stirred for 24 hours at the same temperature. The solid products (Epoxy-LPMSN) were centrifuged, washed with toluene and methanol for three times and dried. The next step is to graft PEI onto the Epoxy-LPMSN: 80 mg of epoxy modified particles were mixed with 200 mg PEI (10 kDa) in 100 ml of carbonate buffer (50 mM, pH 9.5) for 24 hours at room temperature. After this step, the solid product was produced and washed with 20 ml of 1.0 M NaCl and water for three times, and then centrifuged. At the final stage, the solid products were suspended in 20 ml of 1.0 M ethanolamine (pH 9) and stirred at room temperature for 6 hours to block unreacted epoxy groups. The solids were again washed with 20 ml of 1.0 M NaCl and 20 mL water.

Adsorption of Chloroquine into PDMAEA-LPMSN

100 mg of A-MSN was mixed with 80 ml of chloroquine (Chl) solution (100 mg/ml). The suspension was incubated for 24 hours at room temperature under a constant stirring. Suspension was then separated by a centrifugation. Before and after incubation Chl concentration were determined using UV-vis at a wavelength of 329 nm. The difference in Chl amount is determined as the amount of Chl absorbed on the material. The adsorption was then followed by PDMAEA attachment onto Chl loaded A-MSN. The sample is denoted Chl- PDMAEA-LPMSN.

Oligo DNA adsorption and release analysis

Oligo DNA was complexed with PDMAEA-LPMSN (or PEI-LPMSN) at 2 different nitrogen to phosphorous ratio (N/P) (N/P =1 and 10). The complex was mixed in 25 µl of water for 30 minutes at room temperature. Oligo DNA and LPMSN-oligo DNA were used as controls. Agarose gel retardation assay was initiated by adding 5 µl DNA loading dye into the complex which then loaded into a 2% agarose gel containing TAE buffer and stained with ethidium bromide. The gels were run in 1 x TAE buffer for around 10 minutes at 80 V and then followed by observation under a Bio-Rad UV transiluminator.

Cytotoxicity test

The cytotoxicity of PDMAEA-LPMSN and Chl-PDMAEA-LPMSN in KHOS cells were tested by Cell-Titer Glo assay. KHOS cells were seeded in a 96-well cell culture plate with a density of 5×10^3 cells/well. After incubation for 24 hours, the cells were treated with different concentrations of PDMAEA-LPMSN and Chl-PDMAEA-LPMSN solution, followed by further incubation at 37 °C for 48 hours. The cell viability of KHOS cells was evaluated using Cell-Titer Glo assay, according to the protocol provided by the manufacturer. The cells incubated in the absence of particles were used as the control. All the experiments were performed in triplicates for each group. The statistical data were shown as mean ±(SD).

Cellular Uptake (Confocal Microscopy)

KHOS cells were maintained in Dulbecco's Modified Eagle Medium (DMEM) supplemented with fetal calf serum (10%), L-glutamine (2%), penicillin (1%), streptomycin (1%) in 5% CO2 at 37 °C. The medium was routinely changed every 2 days and the cells were separated by trypsinisation before reaching confluency. KHOS cells were seeded in a 6-well plate (1×10^5 cells per well) and incubated for 24 hours prior to cell uptake assay. 50 µg of PDMAEA-LPMSN or Chl-PDMAEA-LPMSN and 2 µl of 100 µM Cy3-oligoDNA was mixed in 100 µl of phosphate buffered saline (PBS) solution and incubated at 4°C overnight. After incubation, the mixture was added to a well of 6-well plates containing 2.0 ml of serum-free DMEM medium, and the final concentration of nanoparticles and Cy3-oligoDNA was 25µg/ml and 100nM, respectively. After incubation for 4 hours at 37°C, the cells washed twice with PBS to remove the remaining nanoparticles, free Cy3-oligoDNA and dead cells. For fixed cell imaging, the cells were treated with 500 µl of 4% PFA PBS solution for 30 minutes at 4 °C, and their nuclei were stained with DAPI for 10 minutes. Finally, the cells were observed under a confocal microscope (LSM Zeiss 710).

siRNA function

To examine whether the particles (PDMAEA-LPMSN and Chl-PDMAEA-LPMSN) can deliver functional molecules to cells for therapy, we chose siRNAs against human PLK1 genes (PLK1-siRNA). An ineffective siRNA, S10-siRNA, was chosen as a negative control because S10-siRNA is effective only against human papillomavirus (HPV) type E6 gene while there is no HPV in KHOS cells. The cells were seeded at 5×10^3 cells / well in 100 µl of complete DMEM medium in 96-well plate and culture for overnight before treatment. The siRNAs were

absorbed to particles as described above (for 21-nucleotide oligo DNA adsorption) and were added to the cells. The cells were treated for 48 hours and the silencing effect or cell viability was determined by Cell-Titer Glo assay.

Characterization

Transmission electron microscopy (TEM) images were obtained by a JEOL 1010 electron microscope with an acceleration voltage 100 kV. Scanning electron microscopy (SEM) images were recorded on a JEOL 6300 microscope operated at 5-10 kV. Nitrogen sorption isotherms of the samples were obtained using a Quantachrome's Quadrasorb SI analyser at 77 K. Before the measurements, the samples were degassed overnight at 110 °C in vacuum. The Brumauer-Emmett-Teller (BET) surface area was calculated using experimental points at a relative pressure of P/P_0 = 0.05-0.25. The total pore volume was calculated from the N_2 amount adsorbed at the highest P/P_0 (P/P_0 = 0.99). The pore size distribution was calculated by the Broekhoff-de Boer (BdB) method using a spherical model. The cavity pore size and entrance pore size are determined from the adsorption and desorption branches, respectively, using the BdB method. XPS spectra were recorded on a Kratos Axis Ultra with a monochromatic Al K_α X-ray source. Each spectrum was recorded at a survey scan from 0 to 1200 eV with a dwell time of 100 ms, pass energy of 160 eV at steps of 1eV with 1 sweep. A high resolution scan was conducted at a lower pass energy (20 eV), higher sweep and dwell time at 250 ms. C1s with a binding energy of 285 eV was used as the reference. The atomic ratio of LPMSN and their functionalised forms (A-MSN and PDMAEA-LPMSN) were determined from XPS spectra and elemental analysis. Solid state magic-angle spinning (MAS) ^{13}C nuclear magnetic resonance (NMR) measurements were performed with a Bruker MSL-300 spectrometer operating at a frequency of 75.482 MHz for ^{13}C. The spectrometer was equipped with a 4-mm double air bearing, magic angle spinning probe for MAS experiments. The proton 90° pulse time used in the CPMAS method was 5.5 µs, the acquisition time was 45 ms, cross-polarisation time 2 ms and the relaxation delay was 3 s. The spectrum width was 50 kHz, and 4000 data points were collected over 2000 scans. Chemical shift of the ^{13}C spectrum was referenced to the resonance of adamantine at 38.23 ppm. All samples were equilibrated at room temperature (22 °C). Zeta potential measurements were conducted on a Zetasizer Malvern Instrument. TGA/DSC 1 (Mettler-Toledo AG) was used for thermogravimetric analysis (TGA) at a heating rate of 2 ºC/min under a nitrogen flow of 20 ml/min.

Results and Discussion

Fig. 1A shows a spherical like morphology of LPMSN with particle sizes around 100 – 200 nm. The spherical morphology in submicron size can also be confirmed from SEM analysis (Fig. 2). The nitrogen sorption analysis of LPMSN demonstrates a type IV isotherm with H2 hysteresis loop at high relative pressure indicating the existence of large mesopores with cage-like structure (Fig. S1). The cavity size of LPMSN was determined to be 11 nm. The main characteristic of LPMSN is its cubic pore structure with a high degree of pore interconnectivity allowing superior mass transfer compared to one-dimensional channel-like structures. This structure also makes the nanoparticles more resistant to pore blocking. [7, 15]

PDMAEA (M_n ~ 4200) (Fig. S2A) was attached to LPMSN through a linking azide silane agent (250 Da, Fig. S2B). TEM image of PDMAEA-LPMSN (Fig.1B) reveals that the functionalization process does not affect the cubic pore structure. The elemental analysis (EA) indicates that there is an increase in the atomic percentage of nitrogen (N) after azide attachment to 1.05 %. The nitrogen content on the surface of LPMSN was also detected by XPS analysis with an atomic ratio of 1.33% (Table 1). Similar results are also confirmed after PDMAEA attachment. There are significant increases in the C and N percentage after the polymer attachment. The carbon composition rose from 6.9% to

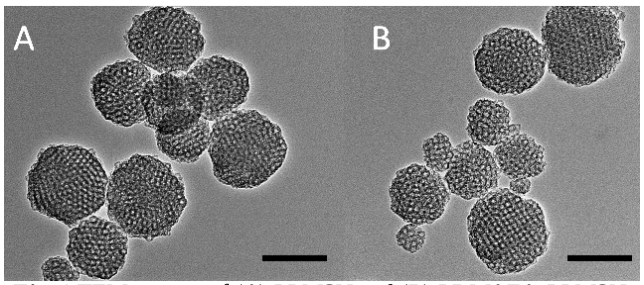

Fig. 1 TEM images of (A) LPMSN and (B) PDMAEA-LPMSN (Scale bar: 100 nm)

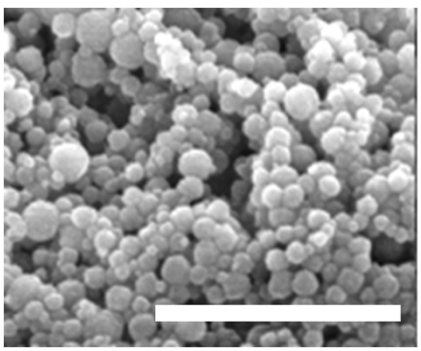

Fig. 2 SEM image of LPMSN (Scale bar: 1 µm)

15.5 % and 13.6% to 59.5% for EA and XPS analysis subsequently. On the other hand, nitrogen concentration increased to 3.5% and 5.1% for EA and XPS analysis. TGA analysis confirms that around 5% weight of azide and 16% weight of PDMAEA have been grafted onto LPMSN (Fig. S3).

Table 1. Chemical composition of composite PDMAEA-LPMSN

	Elemental Analysis			XPS			
	% N	% C	% H	% N	% C	% O	% Si
LPMSN	-	7.54	1.68	-	12.25	62.27	25.47
A-MSN	1.05	6.99	1.59	1.33	13.62	59.18	25.87
PDMAE-LPMSN	3.47	15.5	2.86	5.12	59.55	28.77	6.55

The details of surface modification occurred on the silica materials can be seen from the XPS analyses of N1s for A-MSN and PDMAEA-LPMSN (Fig. S4). Fig. S4A is a typical N1s spectrum for azide moiety. There are two peaks representing N^+ species and N^- species.[28] After PDMAEA attachment, only one single peak of N1s is observed (Fig. S4B). This indicates that

most of nitrogen atoms of azide groups have reacted with alkyne groups of PDMAEA. Thus only C-N binding from PDMAEA repeating unit can be detected. That is why only one single peak instead of two single peaks is observed.

Furthermore, we use ^{13}C NMR analysis to confirm the successful attachment of PDMAEA and to reveal the molecular structure of PDMAEA-LPMSN. Fig. 3 shows the solid state ^{13}C CP-MAS-NMR spectrum of PDMAEA-LPMSN. The peaks at 9.5 ppm (C^1) represent the covalent attachment of PDMAEA onto LPMSN through azide silane bridges. The peaks of C^5, C* and C^7 confirm the successful binding between azide groups and alkyne groups of PDMAEA.[29, 30] The chemical shifts of the ^{13}C NMR resonances of the PDMAEA-LPMSN samples are compiled in Table 2. The chemical bindings can be revealed and attributed to the structure of PDMAEA. In addition, the introduction of PDMAEA produced positive charges on the silica surface, resulting in a positive PDMAEA-LPMSN potential value (+20 mV as compared to LPMSN with -14.0 mV).

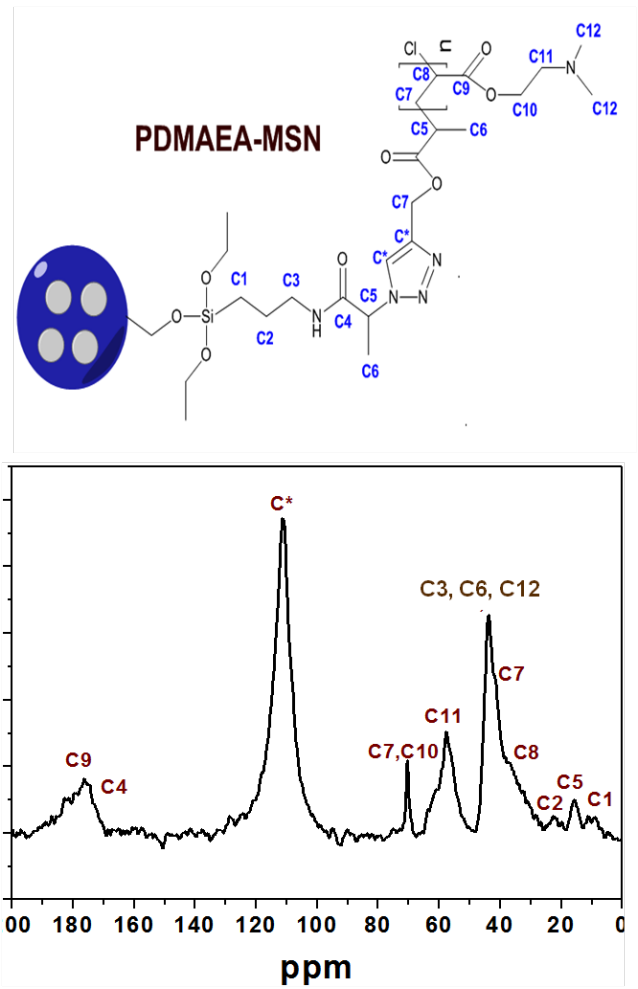

Fig. 3 ^{13}C NMR of PDMAEA-LPMSN

Table 2. Summary of resonance of ^{13}C CP NMR spectra for PDMAEA-LPMSN

PDMAEA-LPMSN	C^1	C^2	C^3	C^4	C^5	C^6	C^7
Chemical Shift (ppm)	9.5	22.7	43.9	174.0	15.9	43.9	42.0
PDMAEA-LPMSN	C^8	C^9	C^{10}	C^{11}	C^{12}	C^*	
Chemical Shift (ppm)	38.0	176.3	70.5	57.7	43.9	111.3	

Fig. S1 shows nitrogen sorption profile of LPMSN, A-MSN and PDMAEA-LPMSN. The azide attachment only gives minor effect on the surface area, pore volume and pore size. The values are similar to LPMSN. For both samples (LPMSN and A-MSN), the surface area were around 400 m^2g, the pore volume at ~ 0.7 cc/g and cavity size at around 11 nm (Table S1). However, the attachment of PDMAEA affected the physical properties. The BET surface area and pore volume values were reduced quite significantly to 105 m^2/g and 0.32 cc/g. We propose that the high percentage of polymer (16% measured from TGA) grafted onto the pore surface and subsequent pore entrance blockage is responsible for such reduction.

We designed PDMAEA to be specifically attached on the MSN surface and not in the pores of MSN. This makes the internal pores which contain hydroxyl group to be accessible for drug molecules. For this reason, initially azide silane was grafted onto as-synthesized silica materials through sylilation reaction. The blocked pores of as-synthesized MSN ascertain azide moieties only attach on the external surface.[31] After surfactant removal, azide-MSN (A-MSN) was connected to PDMAEA through a click reaction.[29, 32] PDMAEA contains alkyne moieties which can chemically react with azide groups. The nitrogen sorption analysis (Fig. S1) confirms that the attachment of azide only occurs on the external surface and do not affect the pore volume or size of the original LPMSN.

To determine the binding and release of oligo DNA (mimic of siRNA) after conjugation with PDMAEA-LPMSN, we performed agarose gel retardation assay for PDMAEA-LPMSN at different incubation time (1 and 2 days). Fig. 4 shows the assay for PDMAEA-LPMSN and PEI-LPMSN at different N/P ratios (1 and 10) to test the binding efficiency of the nanoparticles. For this experiment, we used two types of PDMAEA-LPMSN (PDMAEA-LPMSN and PDMAEA-LPMSN-X) with different concentrations. PDMAEA-LPMSN-X was designed to contain half of the PDMAEA compared to PDMAEA-LPMSN. As a comparison, we also synthesized a composite of polyethyleneimine (PEI) and LPMSN (PEI-LPMSN). PEI is known to be the most widely used polycationic for gene delivery and has been conjugated with MSN for similar purpose.[8, 12]

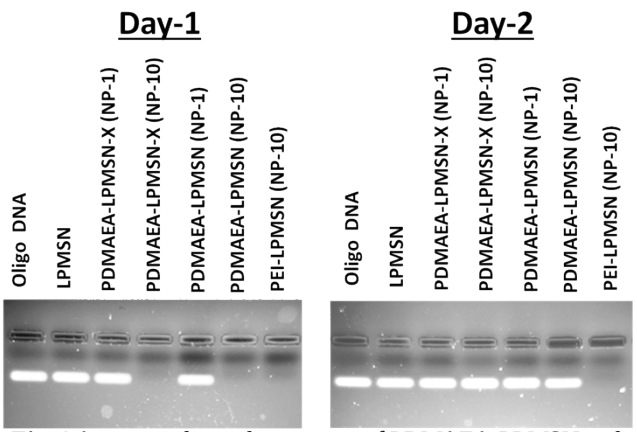

Fig. 4 Agarose gel retardation assay of PDMAEA-LPMSN and PEI-LPMSN after incubation for 30 minutes/Day-1 and after storage for 24 hours/Day-2.

As controls, we used oligo-DNA (lane-1) and LPMSN-oligo-DNA (lane-2). It was expected that the unbound oligo-DNA which was released from the particles can be observed as an emerge band on specific lanes. This band will not be detected as long as the oligo-DNA bind to the nanoparticles.[24] After 30 min incubation, a mark can be observed from incomplete binding of oligo-DNA with PDMAEA-LPMSN and PDMAEA-LPMSN X at N/P =1. In contrast, these marks were not detected in the case of PDMAEA-LPMSN and PDMAEA-LPMSN-X at N/P = 10. These results confirmed that higher N/P ratio is required for better interaction and complete binding of biomolecules. Larger N/P ratio causes a better condensation of complex of PDMAEA and oligo-DNA.[23, 24] Thus, a complex of PDMAEA-LPMSN and oligo-DNA at N/P ratio of 10 performed strong interaction with oligo-DNA and maintained the complex stability.

The stable binding between carrier and oligo-DNA for the first several hours is very important to ascertain the delivery of the siRNA within the cytoplasm.[23, 24] Interestingly, after 24 hours incubation, the smearing can be observed from most of the lane except from PEI-MSN. PEI is known to be very effective in performing complex with plasmid DNA and siRNA. The multiple amine moieties within PEI enable strong interaction with the nucleic acids and cell membrane. Yet, PEI also has some drawback regarding the release of the nucleic acid from the complexes.[16, 17] The strong binding interaction between PEI and biomolecules hinders the release, thus no band is observed from PEI-MSN lane. In contrast, the smearing can be detected from all PDMAEA-LPMSN lanes. In the case of PDMAEA-LPMSN, PDMAEA is capable to maintain its ionic strength for the first few hours before starting to degrade to non-toxic compounds, leading to temporary binding of oligo-DNA. [23, 24] After released from PDMAEA-LPMSN, oligo-DNA can be observed in the gel, in agreement with previous reports. [23, 24] It was found that the polymer can maintain its binding with DNA for a sufficiently long period of time to transfect cells (around 4 hours) and then release the DNA inside the cells after 10 hours.[23, 24] Therefore we choose the PDMAEA-LPMSN composition rather than conventional PEI functionalization in previous studies.

To enhance siRNA delivery, it is important for the carrier to escape from endosomal entrapment and deliver siRNA within cytoplasm. We introduced Chl in the LPMSN's pores, which is also known as endosomal-escape inducing materials.[14, 19]. Chl is weakly basic and can be attracted with negatively charged silanol groups. It is very soluble in water with the solubility up to 1 mg/ml.[14, 33] However, the nature of PDMAEA-LPMSN that can be degraded in water makes the adsorption of Chl into PDMAEA-LPMSN in water impracticable. In addition, the nitrogen sorption shows that most of the entrance pores have been blocked after PDMAEA attachment, suggesting the adsorption of Chl after the polymer attachment is difficult. To optimize Chl adsorption, we designed the adsorption to be conducted after azide attachment (Scheme 1). Following surfactant removal, the pores of azide-MSN were accessible for Chl. The adsorption of Chl onto A-MSN was conducted in water for 24 hours.[33] Then, PDMAEA attachment was carried in toluene. Loading amount of Chl in PDMAEA-LPMSN based on UV analysis was at 100 mg/g (0.1 mg/mg MSN).

Cite this: DOI: 10.1039/c0xx00000x

www.rsc.org/xxxxxx

ARTICLE TYPE

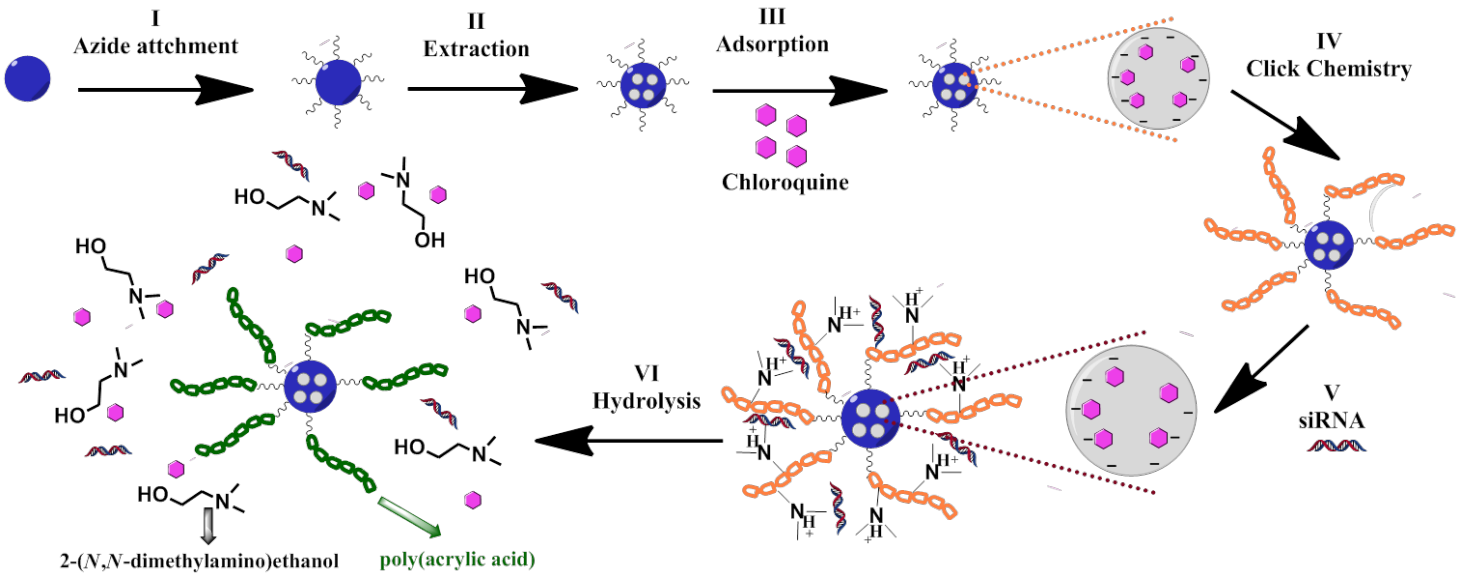

Scheme 1. Detailed mechanism of chloroquine loading and siRNA binding for dual delivery

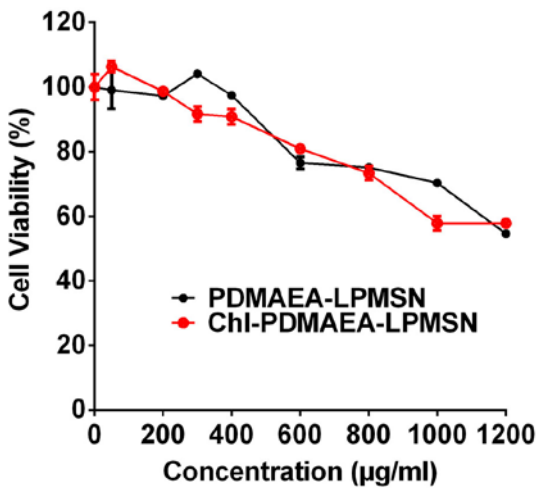

Fig. 5 Cytotoxicity test for PDMAEA-LPMSN and Chl-PDMAEA-LPMSN

As shown in Scheme 1, PDMAEA-LPMSN is designed to co-deliver siRNA and Chl in a controllable manner. After PDMAEA degradation, not only the siRNA can be released, but also the release of Chl is accelerated following the rupture of PDMAEA on the MSN surface, which promotes endosomal escapes of siRNA within cytoplasm. To evaluate the cytotoxicity of the composite materials (PDMAEA-LPMSN and Chl-PDMAEA-LPMSN), we tested the effect of the particle's concentration against KHOS cell viability. Fig. 5 shows that the composite materials induced negligible toxicity even at a very high concentration 400 µg/ml. The half maximal inhibitory concentration (IC_{50}) values of PDMAEA-LPMSN and Chl-PDMAEA-LPMSN were similar, around 1200 µg/ml, which can be explained by the very low toxicity of PDMAEA[23, 24] and unmodified LPMSN.[15]

Similar to PDMAEA-LPMSN, Chl-PDMAEA-LPMSN did not affect the cell viability. This is in agreement with a previous report that showed Chl loaded MSN with a loading amount 0.15 mg/mg (close to Chl-PDMAEA-LPMSN, 0.1 mg/mg) has negligible effect on cytotoxicity.[14] Our findings confirm that both PDMAEA-LPMSN and Chl-PDMAEA-LPMSN are safe to be used even at a high concentration.

Fig. 6 illustrates the cell uptake study of PDMAEA-LPMSN and Chl-PDMAEA-LPMSN. Confocal microscopy was used to observe the internalization of the particles. At first, all particles were conjugated with oligo-DNA, and then incubated with KHOS cell lines. To adequately follow adsorption and the cell internalization process, oligo-DNA was labeled with cyanine dye (Cy3-oligo-DNA) to show red fluorescence. Cy3-oligo-DNA itself without any nano-carriers did not show any red signal coming from Cy3, similar as what observed in the control group without any treatment. The blue signals observed were from DAPI stained nuclei. In contrast, both PDMAEA-LPMSN and Chl-PDMAEA-LPMSN conjugated with Cy3-oligo-DNA reveal

red signal. These results demonstrated that the negatively charged oligo-DNA themselves cannot enter into the cells, while the functional nanoparticles (PDMAEA-LPMSN and Chl-PDMAEA-LPMSN) have the capacity to deliver the genetic molecules into the cells.

The polycation PDMAEA has the interaction with oligo-DNA and also cells membrane, essential for cellular uptake.[8, 15] Compared to PDMAEA-LPMSN, it was observed that Chl-PDMAEA-LPMSN showed stronger and more homogeneous Cy3 signal. It is known that Chl is a DNA intercalator which has preferential binding towards G-C sequence.[34] We propose that Chl located adjacent to the external surface of LPMSN might improve the binding to oligo-DNA molecules. The stronger binding causes more oligo-DNA to be carried and delivered into the cells. After cellular uptake, Chl induce endosomal escape by its buffering capability.[14] Consequently, the red signal coming from Cy3 is distributed homogeneously in the cytoplasm. In contrast, without Chl, the carriers are localised within discrete spot (see also Fig. 6).[34]

The ability of PDMAEA-LPMSN to co-deliver bio-functional siRNA and chloroquine (Chl) was investigated by using PLK1-siRNA against polo-like kinase 1 and testing the cell toxicity in an osteosarcoma cell line KHOS. Fig. 7 confirms that PDMAEA-LPMSN as a carrier has a negligible cell inhibition performance. Our previous study showed that PDMAEA as a single carrier has a low endosomal escape property,[25] indicating that the siRNAs delivered by PDMAEA-LPMSN, similar to PDMAEA, cannot escape from endosomal entrapment to induce silencing effect.[25] In contrast, Chl-PDMAEA-LPMSN induces a reasonably significant decrease in cellular viability (25%). Our results have shown that although the actual benefit of PDMAEA as a single carrier for gene silencing is limited,[25] the conjugation with LPMSN offers more opportunities for the fabrication of effective and multi-functional nano-carriers.

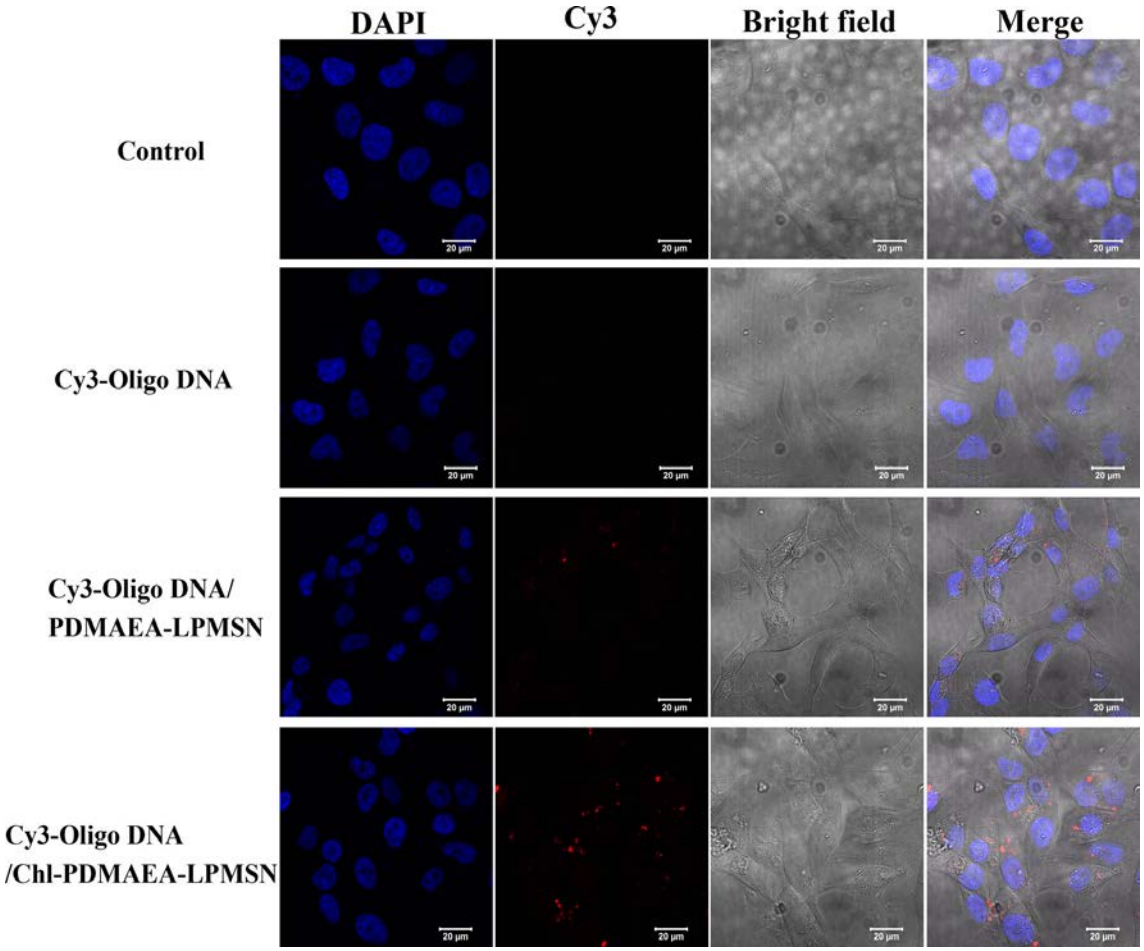

Fig. 6 Assessments of cell uptake by confocal microscopy**.** The cell uptake efficiency of PDMAEA-LPMSN and Chl-PDMAEA-LPMSN were examined by labeling the particles with a 21-nt oligo DNA conjugated with Cy-3.

Cite this: DOI: 10.1039/c0xx00000x

www.rsc.org/xxxxxx

ARTICLE TYPE

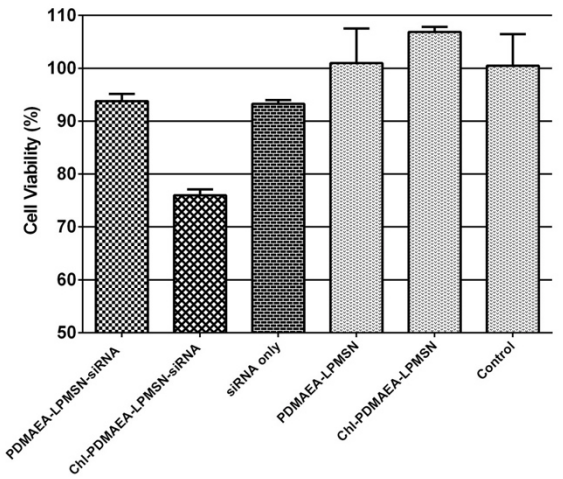

Fig. 7 Biological function analysis of PDMAEA-LPMSN and Chl-PDMAEA-LPMSN by delivering PLK1 siRNA in KHOS cells.

Conclusion

In this study, a novel gene carrier with selected properties: degradable, low toxicity and high capacity was prepared by grafting "self-catalyzed degradation" PDMAEA onto the surface of large pore and cubic mesostructured mesoporous silica nanoparticle to produce an efficient gene carrier: PDMAEA-LPMSN. The composite materials have very low toxicity even at a very high concentration of 400 μg/ml. The degradable PDMAEA enables the release of siRNA after endocytosis. The chloroquine loaded inside the nanopores allows the cargo molecules escape from endosomal entrapment. These results demonstrate the potential of PDMAEA-LPMSN as a gene carrier. To fully use the potential of PDMAEA-LPMSN, it is expected that chemotherapy drugs can also be loaded, offering multi-functional nano-carriers for dual delivery applications.

Acknowledgements

We thank the Australian Research Council for financial support. We acknowledge the Australian National Fabrication Facility and the Australian Microscopy & Microanalysis Research Facility at the Centre for Microscopy and Microanalysis, The University of Queensland and Dr. Barry Wood from The Brisbane Surface Analysis Facility for support in XPS analysis and Dr. Ekaterina Strounina from Centre for Advanced Imaging for NMR analysis. S.B.H gratefully acknowledges the UQIRTA scholarship from The University of Queensland.

Notes and references

[a] *Australian Institute for Bioengineering and Nanotechnology, The University of Queensland, Brisbane, QLD 4072, Australia.*
[b] *School of Chemical Engineering, The University of Adelaide, Adelaide, Australia*
* Email: m.monteiro@uq.edu.au; s.qiao@adelaide.edu.au; c.yu@uq.edu.au

†Electronic Supplementary Information (ESI) available: Nitrogen sorption and TGA analysis of LPMSN, A-MSN and PDMAEA-LPMSN; High resolution XPS analysis for A-MSN and PDMAEA-LPMSN. See DOI: 10.1039/b000000x/

1. C. R. Sibley, Y. Seow and M. J. A. Wood, *Mol. Ther.*, 2010, **18**, 466-476.
2. D. Reischl and A. Zimmer, *Nanomedicine*, 2009, **5**, 8-20.
3. B. Ozpolat, A. K. Sood and G. Lopez-Berestein, *J. Intern. Med.*, 2009, **267**, 44-53.
4. X. Gao and L. Huang, *Biochemistry*, 1996, **35**, 1027-1036.
5. I. Ojea-Jimenez, L. Garcia-Fernandez, J. Lorenzo and V. F. Puntes, *ACS Nano*, 2012, **6**, 7692-7702.
6. S. Jiang, A. A. Eltoukhy, K. T. Love, R. Langer and D. G. Anderson, *Nano Lett.*, 2013, **13**, 1059-1064.
7. F. Gao, P. Botella, A. Corma, J. Blesa and L. Dong, *J. Phys. Chem. B*, 2009, **113**, 1796-1804.
8. T. Xia, M. Kovochich, M. Liong, H. Meng, S. Kabehie, S. George, J. I. Zink and A. E. Nel, *ACS Nano*, 2009, **3**, 3273-3286.
9. X. He, K. Wang, W. Tan, B. Liu, X. Lin, S. Huang, D. Li, C. He and J. Li, *Chin. Sci. Bull.*, 2003, **48**, 223-228.
10. M.-H. Kim, H.-K. Na, Y.-K. Kim, S.-R. Ryoo, H. S. Cho, K. E. Lee, H. Jeon, R. Ryoo and D.-H. Min, *ACS Nano*, 2011, **5**, 3568-3576.
11. H.-K. Na, M.-H. Kim, K. Park, S.-R. Ryoo, K. E. Lee, H. Jeon, R. Ryoo, C. Hyeon and D.-H. Min, *Small*, 2012, **8**, 1752-1761.
12. H. Meng, M. Liong, T. Xia, Z. Li, Z. Ji, J. I. Zink and A. E. Nel, *ACS Nano*, 2010, **4**, 4539-4550.
13. A. M. Chen, M. Zhang, D. Wei, D. Stueber, O. Taratula, T. Minko and H. He, *Small*, 2009, **5**, 2673-2677.
14. S. R. Bhattarai, E. Muthuswamy, A. Wani, M. Brichacek, A. L. Castaneda, S. L. Brock and D. Oupicky, *Pharm. Res.*, 2010, **27**, 2556-2568.
15. S. B. Hartono, W. Gu, F. Kleitz, J. Liu, L. He, A. P. J. Middelberg, C. Yu, G. Q. Lu and S. Z. Qiao, *ACS Nano*, 2012, **6**, 2104-2117.

16. G. Lin, R. Hu, W.-C. Law, C.-K. Chen, Y. Wang, H. L. Chin, Q. T. Nguyen, C. K. Lai, H. S. Yoon, X. Wang, G. Xu, L. Ye, C. Cheng and K.-T. Yong, *Small*, 2013, Ahead of Print.
17. A. A. Eltoukhy, D. Chen, C. A. Alabi, R. Langer and D. G. Anderson, *Adv. Mater.*,2013, **25**, 1487-1493.
18. D. M. Dykxhoorn, C. D. Novina and P. A. Sharp, *Nat. Rev. Mol. Cell Biol.*, 2003, **4**, 457-467.
19. M. Wang, X. Li, Y. Ma and H. Gu, *Int. J. Pharm.*, 2013, **448**, 51-57.
20. B. Chang, D. Chen, Y. Wang, Y. Chen, Y. Jiao, X. Sha and W. Yang, *Chem. Mater.*, 2013, **25**, 574-585.
21. R. Namgung and W. J. Kim, *Small*, 2012, **8**, 3209-3219.
22. C. A. Hong, J. S. Kim, S. H. Lee, W. H. Kong, T. G. Park, H. Mok and Y. S. Nam, *Adv. Funct. Mater.*, 2013, **23**, 316-322.
23. N. P. Truong, Z. Jia, M. Burges, N. A. J. McMillan and M. J. Monteiro, *Biomacromolecules*, 2011, **12**, 1876-1882.
24. N. P. Truong, Z. Jia, M. Burgess, L. Payne, N. A. J. McMillan and M. J. Monteiro, *Biomacromolecules*, 2011, **12**, 3540-3548.
25. N. P. Truong, W. Gu, I. Prasadam, Z. Jia, R. Crawford, Y. Xiao and M. J. Monteiro, *Nat Commun*, 2013, **4**, 1902.
26. Y. Han and J. Y. Ying, *Angew. Chem., Int. Ed.*, 2005, **44**, 288-292.
27. V. Percec, T. Guliashvili, J. S. Ladislaw, A. Wistrand, A. Stjerndahl, M. J. Sienkowska, M. J. Monteiro and S. Sahoo, *J. Am. Chem. Soc.*, 2006, **128**, 14156-14165.
28. D. A. Egede, S. Hvilsted, T. S. Hansen and N. B. Larsen, *Macromolecules*, 2008, **41**, 4321-4327.
29. J. Nakazawa, B. J. Smith and T. D. P. Stack, *J. Am. Chem. Soc.*, 2012, **134**, 2750-2759.
30. A. Schlossbauer, D. Schaffert, J. Kecht, E. Wagner and T. Bein, *J. Am. Chem. Soc.*, 2008, **130**, 12558-12559.
31. L. Xu, F. Xu, F. Chen, J. Yang and M. Zhong, *J. Nanomater.*, 2012, 457967, 457910 .
32. N. Moitra, P. Trens, L. Raehm, J.-O. Durand, X. Cattoen and M. W. C. Man, *J. Mater. Chem.*, 2011, **21**, 13476-13482.
33. V. Sanz, C. Tilmaciu, B. Soula, E. Flahaut, H. M. Coley, S. R. P. Silva and J. McFadden, *Carbon*, 2011, **49**, 5348-5358.
34. S. Yang, D. J. Coles, A. Esposito, D. J. Mitchell, I. Toth and R. F. Minchin, *J. Controlled Release*, 2009, **135**, 159-165.